Chaotic Random Neural Networks
BIO 438: Computational Neuroscience

Hania Shahid
24100044

1 Introduction

In this exposition, we look into two different mathematical formalism of modeling the mean-field theory (MFT) of random neural networks. The mean field theory is based on the idea of approximating the behavior of a large network of neurons by assuming that each neuron behaves independently of the others and is influenced only by the average activity of the rest of the population. By modeling each neuron as a rate unit that, when averaged over the entire population of neurons, represents the average firing rate in a field of neurons with similar properties. What we mean by random in the case of random neural networks is that each neuron in the population is regarded as an object with an associated random weight in the bifurcation of its pre-synaptic and post-synaptic coupling.

The mean-field theory for recurrent networks of rate units typically involves a set of differential equations that describe the dynamics of the network's firing rates over time. We access solutions after a given time, such that the system is assumed to reach a satisfactory steady state. These equations take into account the connectivity between neurons and the strength of the synaptic connections, as well as external inputs to the network.

We will be following carefully the calculations done in [1], as well as the more rigorous and improved approach in [2] which using path integrals to systematically model the dynamic mean field equations that are more capable of deriving in general the stability of the derived mean field equations, and they are amenable to analysis of finite size corrections.

The focus here is to model dynamical systems of large populations of neurons, namely where $N \to \infty$ in a deterministic non-linear system, under the assumption that the distribution of firing rates approaches a continuous function. To ensure that the system is in fact random, the weight to the coupling of one neuron to the other will be done using a Gaussian random variable. Since the degrees of freedom are this infinite, we will show that in this limit, the system transitions from a stationary state to a chaotic state The time-varying self-consistent mean-field theory explains both the statistical characteristics of the chaotic flow and its transition.

2 Formalism

Consider N localized continuous variable (these represent individual neurons), and $S_i(t), i = 1, \ldots, N$ to be the firing rate of each neuron. Associated with each neuron is a field (its membrane potential), h_i, $-\infty < h_i < +\infty$, which is related to the firing rate as

$$S_i(t) = \phi(gh_i(t)), \tag{2.1}$$

where the constant $g > 0$ is a measure of the nonlinearity of the system, representing slope of the linear response of the neuron to small post-synaptic potential. and $\phi(x)$ is a gain function that models the input-output behavior of the neurons (i.e. it relates h_i to S_i). We assume $\phi(x)$ to be a sigmoid function: $\phi(\pm\infty) =$

± 1, $\phi(-x) = -\phi(x)$. A sigmoid function (shown in figure below) is one that maps any input value to a value between 0 and 1. It is characterized by an S-shaped curve that rises gradually at first, then more steeply, before leveling off at the upper limit of 1.
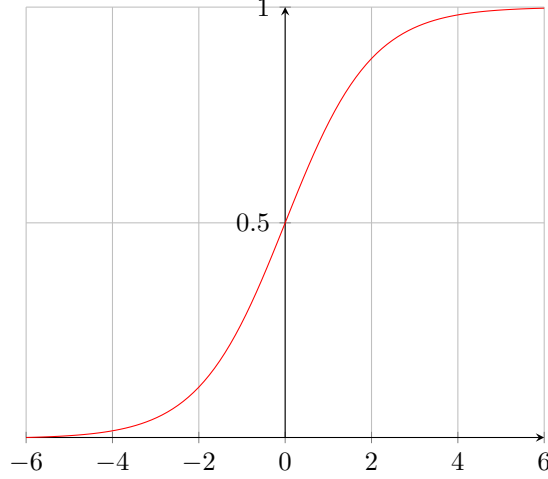
For the sake of concreteness, we model $\phi(x)$ as

$$\phi(x) = \tanh(x), \tag{2.2}$$

We can then write N first-order differential equations to represent the dynamics of the neural network:

$$\dot{h}_i = h_i + \sum_{j=1}^{N} J_{ij} S_j = h_i + \sum_{j=1}^{N} J_{ij} \phi(g h_j) \tag{2.3}$$

where J_{ij} couples the jth neuron's output to the input of the ith neuron; $J_{ii} = 0$, which means that an individual neuron cannot receive any of its own output as input. We consider a non-symmetric matrix $\mathbf{J}$:

$$J_{ij} = \begin{pmatrix} 0 & a_{12} & a_{13} & \cdots & a_{1n} \\ a_{21} & 0 & a_{23} & \cdots & a_{2n} \\ a_{31} & a_{32} & 0 & \cdots & a_{3n} \\ \vdots & \vdots & \vdots & \ddots & \vdots \\ a_{n1} & a_{n2} & a_{n3} & \cdots & 0 \end{pmatrix} \tag{2.4}$$

The long time behavior of the system can depend on the particular values of J_{ij}'s. Since we want random synaptic coupling, each of J_{ij} is an independent variable having a random Gaussian distribution. It then follows that $\langle J_{ij} \rangle = 0$ and $\langle J_{ij}^2 \rangle - \langle J_{ij} \rangle^2 = J^2/N$. We can thus replace g in equation 2.1 with the gain parameter gJ.

2.1 Dynamical Mean Field Theory

The behaviour of the solutions to equations 2.3 after long time periods have been explored using the dynamical mean field theory (DMFT) for large values of N, which was originally created for studying spin glasses [3]. This approach becomes exact in the limit where $N \to \infty$. For $t \gg 1$, the dynamics of the system can be simplified into the self-consistent equation of an individual neuron:

$$\dot{h}_i(t) = -h_i + \eta_i(t), \tag{2.5}$$

2

where t represents time and η_i is a time-dependent Gaussian field, from the random inputs of other neurons, as in the last term in equation 2.3. The variance can be determined from 2.3 as well to be

$$\langle \eta_i(t)\eta_i(t+\tau)\rangle = J^2 C(\tau), \tag{2.6}$$

where $C(\tau)$ is the average auto-correlation function and is calculated, using equations 2.2 and 2.5 to be the following:

$$C(\tau) = \langle \phi(h_i(t))\phi(h_i(t+\tau))\rangle. \tag{2.7}$$

where the average has been carried out over the distribution of **J**. Here, The properties of an auto-correlation function are that it tells (i) how correlated the signal is with itself at different time lags and (ii) how dependent future values of the signal are on past values. In deriving equation 2.6, we have assumed that the system reached a steady state and so the correlations depend only on time separations, and that $C(t) = C(-t)$. For the sake of convenience, let us solve the differential equation for the local field auto-correlation where there is approximately no gain parameter change; the new auto-correlation function is therefore

$$\Delta(\tau) = \langle h_i(t)\rangle\, h_i(t+\tau) \tag{2.8}$$

which obeys the relation $\Delta - \ddot{\Delta} = J^2/C$. $\Delta(t)$ must be a differentiable even function and must be bounded by $|\Delta(t)| \leq \Delta(0)$. We can then arrive to the expression

$$\ddot{\Delta} = \frac{\partial V}{\partial \Delta}. \tag{2.9}$$

where $V(\Delta)$ can be understood to be a Newtonian potential causing one-dimensional motion in $\Delta(t)$.

The calculation for this is as follows: we begin by integrating both sides of equation 2.5 from t to ∞:

$$h_i(t) = \int_{t'}^{\infty} \eta_i(t')e^{-(t'-t)}dt' \tag{2.10}$$

Taking the expectation value of both sides:

$$\langle h_i(t)\rangle = J^2 \int_{t'}^{\infty} C(t'-t'')e^{-(t'-t)}dt' \tag{2.11}$$

Using the defined function in 2.8, we evaluate the expectation value:

$$\Delta(\tau) = \left[J^2 \int_{t'}^{\infty} C(t'-t)e^{-(t'-t)}dt' \right] \int_{t''}^{\infty} C(t''-t-\tau)e^{-(t''-t-\tau)}dt'' \tag{2.12}$$

Assuming the potential V depends only on Δ, $V = V(\Delta)$, and thus taking the functional derivative of V with respect to Δ:

$$\frac{\delta V}{\delta \Delta} = \frac{\partial V}{\partial \Delta} \tag{2.13}$$

Equating this to the l.h.s of equation 2.5 gives:

$$\frac{\partial V}{\partial \Delta} = \frac{d\langle h_i(t)\rangle}{dt} \tag{2.14}$$

The potential V takes the form

$$V = -\frac{1}{2}\Delta^2 + \int_{-\infty}^{\infty} Dz \left(\int_{-\infty}^{\infty} Dx\; \Phi(\sqrt{(\Delta(0)-|\Delta|)}x + \sqrt{|\Delta|}z) \right)^2 \tag{2.15}$$

where $Dz = dz \exp(-z^2/2)/\sqrt{2\pi}$ and $\Phi(x) = \int_0^x \phi(y)$. The potential depends on $\Delta(0)$, which is determined by equation 2.9.

3

2.2 The Path Integral Approach

We now move onto another framework to study the dynamical properties of neural network, using path integrals [2]. We continue to use the same general notation as before, and any new variables will be defined accordingly.

Let us focus on the network's equilibrium state, the dynamical state where the network eventually settles after a sufficient amount of time has elapsed since the initial time t_0. Thus, we will assume that $t_0 \to -\infty$ so that the initial state at t_0 is no longer relevant or remembered. The matrix $\mathbf{J}$ (2.4) is studied in its non-symmetric form once again, meaning $J_{ij} \neq J_{ji}$; in this pretext also, we find some unexpected behavior in the system, such as fix points, limit cycles, and chaotic behavior. Consider a fully connected network with random, asymmetric and independent couplings:

$$\bar{J}_{ij} = 0, \ \bar{J}_{ij}^2 = 1/N, \ \overline{J_{ij}J_{ji}} = 0 \tag{2.16}$$

where the bar denotes averaging with the coupling probability distribution $P(\mathbf{J}) = \prod_{ij} P(J_{ij})$. The matrix elements J_{ij} are once again independent and identically distributed Gaussian variables.

We begin by re-writing equation 2.3 in a more sophisticated manner:

$$\partial_a h_i^a = -h_i^a + \sum_{j=1}^{N} J_{ij} S_j^a \tag{2.17}$$

where $\partial_a = (d/dt_a) + \delta(\delta \to 0^+)$ to ensure causality by enforcing that derivatives only depend on past values and not future values; and $S_j^a = \phi(gh_j^a)$. To convert the continuous variables into a finite dimensional space, we divide the time interval being considered $[t_0, t]$ into n segments of length δt and change the differential into a finite-difference equation by making the replacement $\partial_a h_i^a = f(h_i^a)$. The equation 2.17 then becomes:

$$h_i^{a+1} - h_i^a = f(h_i^a)\delta(t) + b_i^a\delta(t) + h_i^0\delta_{a0}^{\mathrm{Kr}} \tag{2.18}$$

where the Kronecker delta $\delta_{a0}^{\mathrm{Kr}}$ is used to enforce the initial condition and $a = 0, 1, \ldots, n$ is a discrete index which labels the time slices. The term b_i^a is an external field term to evaluate output from other neurons. The reason we discretize the differential is so that we may consider all possible "paths" or trajectories that the system could take between the two states, and add up (integrate the probability amplitude for each path; this can be visualized as in figure 1.

If $\tilde{h}_i^a$ is the solution to equation 2.18, then we get the correlation function

$$Z[\hat{b}, b] = \int \prod_a \prod_i dh_i^a \ \delta\left(h_i^a - \tilde{h}_i^a\right) \ e^{-i\hat{b}_a^i h_a^i} \tag{2.19a}$$

$$= \int \prod_a \prod_i dh_i^a \ \delta\left(h_i^{a+1} - h_i^a - f(h_i^a)\delta(t) - b_i^a\delta(t) - h^0 i\delta_{a0}\right) e^{-i\hat{b}_a^i h_a^i} \tag{2.19b}$$

We obtain 2.19b by using the identity $\delta(h_i^a - \tilde{h}_i^a) = |F'(h_a^i)| \ \delta F(h_a^i)$ where $F'(h_a^i)$ is the Jacobian of the transformation $(h_i^a - \tilde{h}_i^a) = 0 \to F(h_a^i) = 0$.

Even in the limit of an infinitely fine discretization ($n \to \infty$), where the numerical solution should approach the true continuum solution, the discretization scheme still affects the resulting finite difference equations. Apart from the initial values of the response functions (which do depend on the discretization), the Jacobian ensures that the final correlators and response functions are independent of the discretization details and match the theoretical continuum predictions. The role of the Jacobian is thus to cancel out the discretization
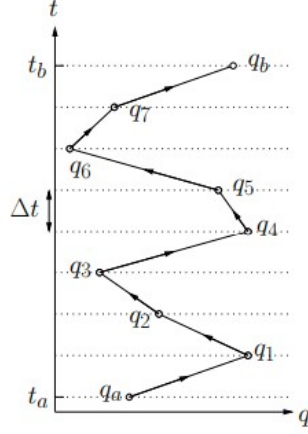
4

Figure 1: Discrete approximation to a path. Each path is specified by $N-1$ numbers $q_1(t), \ldots, q_{N-1}(t)$. To sum over paths, we must integrate each $q_i(t)$ from $-\infty$ to $+\infty$. Once all integrations are done, we can take the limit $N \to \infty$ [4].

scheme dependence, resulting in generating functional evaluations that yield the correct continuum physics. Without the Jacobian, the results would reflect an unwanted influence from the numerical discretization.

The expression 2.19b can be simplified by using the Fourier representation of the Dirac δ-function

$$\delta(z_i^a) = \int_{-\infty}^{+\infty} \frac{d\hat{h}_i^a}{2\pi} \, e^{-i\hat{h}_i^a z_i^a} \tag{2.20}$$

and rewritten as

$$Z[\hat{b}, b] = \int \prod_a \prod_i \frac{d\hat{h}_i^a dh_a^i}{2\pi} \times e^{-i\hat{h}_i^a (h_i^{a+1} - h_i^a - f(h_i^a)\delta t - b_i^a \delta t - h_i^0 \delta_{a0}) + i\hat{b}_i^a h_i^a} \tag{2.21}$$

Taking the continuum limit $n \to \infty$ with $n\delta t = t - t_0$, $Z[\hat{b}, b]$ becomes a path integral over all possible paths $\{\hat{h}_i, h_i\}_{t_a \in [t_0, t]}$. We then get

$$Z[\hat{b}, b] = \int \prod_i \mathcal{D}\hat{h}_i \, \mathcal{D}h_i \, e^{-S[\hat{h}, h] + \sum_{ia}(\hat{b}_i^a h_i^a + i\hat{h}_i^a b_i^a)} \tag{2.22}$$

where

$$\mathcal{D}\hat{h}_i = \lim_{n \to \infty} \prod_a \frac{d\hat{h}_i^a}{2\pi},$$

$$\mathcal{D}h_i = \lim_{n \to \infty} \prod_a dh_i^a, \text{ and}$$

$$S[\hat{h}, h] = \sum_{ia} \hat{h}_i^a \Big(\partial_a h_i^a + h_i^a - \sum_j J_{ij} S_j^a - h_i^0 \delta_{a0}\Big)$$

$S[\hat{h}, h]$ is the dynamical action of the equation of motion 2.17 with the initial condition $h_i^0 = h_i^a(t_0)$. The Kronecker thus becomes $\delta_{a0} = (t_a - t_0)$. Hat fields $\hat{h}, \hat{b}$ can be called response fields because we average $Z[\hat{b}, b]$

5

over all trajectory generate by equation 2.17 in the presence of the external field b_i^a. Since $Z[0,0] = 1$, we can obtain average correlation functions by averaging $Z[\hat{b}, b]$ over elements of J_{ij}. This leads to

$$\bar{Z}[\hat{b}, b] = \int \prod_i \mathcal{D}\hat{h}_i \mathcal{D}h_i \exp\left[-\sum_{ia} i\hat{h}_i^a(1 + \partial_a)h_i^a + \frac{1}{2N}\sum_{ij}(\sum_a i\hat{h}_i^a S_j^a)^2 - h_i^0 \delta_{a0} + \sum_{ia}(i\hat{b}_i^a h_i^a + i\hat{h}_i^a b_i^a) \right] \tag{2.23}$$

The inter-connectivity of the system allows us to diagonalize the exponent in equation 2.23 with respect to the site index i. But the auxiliary fields, b and $\hat{b}$ which represent the interactions between sites, still retain a residual component. We now use this and introduce the field $C^{ab} = \sum_i S_i^a S_i^b / N$ to write the averaged generating functional as the following partition function of a dynamical field theory for the fields $\{\hat{C}^{ab}, C^{ab}\}$:

$$\bar{Z}[\hat{b}, b] = \int \mathcal{D}\hat{C}, \mathcal{D}C \; e^{-N\mathcal{L}[\hat{C}, C; \; \hat{b}, b]} \tag{2.24}$$

with $\hat{C}^{ba} = \hat{C}^{ab}$ and $C^{ba}C^{ab}$ and

$$\mathcal{L}[\hat{C}, C; \; \hat{b}, b] = \frac{1}{2} = \sum_{ab}\left(i\hat{C}^{ab}C^{ab} + \frac{\epsilon}{2}\hat{C}^{ab}\hat{C}^{ab} \right) - W[\hat{C}, C; \; \hat{b}, b] \tag{2.25}$$

Note that the functional $W[\hat{C}, C; \; \hat{b}, b]$ is the generating functional of connected (time) correlation functions of h_i and $\hat{h}_i$ generated by the action:

$$\mathcal{L}[\hat{C}, C; \; \hat{b}, b] = \sum_i S[\hat{h}_i, h_i; C, \hat{C}] - \sum_{ia}(i\hat{h}_i^a b_i^a + i\hat{b}_i^a h_i^a) \tag{2.26}$$

If we now consider the limit $N \to \infty$ in the equation 2.24, and take the average over all paths of $\mathcal{L}[\hat{h}, h; \hat{C}, C; \; \hat{b}, b]$ as governed by the stationary-action principle [5], we get the expressions

$$Z_0[\hat{b}, b] = e^{-N\mathcal{L}_0[C, \hat{C}; \hat{b}, b]} \qquad N \gg 1, \tag{2.27}$$

$$\frac{\delta}{\delta i\hat{C}^{ab}}\mathcal{L}[\hat{C}, C; \hat{b}, b] = 0 \implies C^{ab} = \frac{1}{N}\sum_i \langle S_i^a S_i^b \rangle_0 + \epsilon i\hat{C}^{ab} \tag{2.28}$$

Since we can normalize the partition function as $\bar{Z}[0, b] = 1$, then $C^{ab} = 0$ must be the correct self-consistent auto-correlation function. We can then infer that $\bar{Z}[\hat{b}, b] = \prod_i Z_i[\hat{b}, b]$ and therefore the behavior of the entire system can be packaged into the single unit processes $\{\bar{h}_i, \hat{h}_i\}$, under the limit $N \to \infty$. If we consider η^a to be a Gaussian field with a mean of 0, then we can write that

$$\langle \eta^a \eta^b \rangle_\eta = C^{ab} \tag{2.29}$$

using the identity

$$\exp\left[\frac{1}{2}\sum_{ab} i\hat{h}_i^a C^{ab} i\hat{h}_i^b \right] = \left\langle \exp \sum_a i\hat{h}_i^a \eta^a \right\rangle_\eta .$$

The stochastic differential equation is then

$$\partial_a h_i^a + b_i^a + \eta^a \tag{2.30}$$

for which the generating functional is

$$Z_i[\hat{b}, b] = \left\langle \int \mathcal{D}\hat{h}_i \mathcal{D}h^i \; e^{-\sum_a i\hat{h}^a{}_i[(1+\partial_a)h_i^a - \eta^a - h_i^0 \delta_{a0}] + \sum_a (i\hat{h}^a{}_i b_i^a + i\hat{b}_i^a h_i^a)} \right\rangle_\eta . \tag{2.31}$$

In the limit of an infinitely large network $N \to \infty$, this procedure provides a complete description of the network's dynamics. While the formalism diagonalizes the site index i, it retains memory of the inter-dependencies between sites through the Gaussian field η^a. The field η^a captures the effects of the other sites on site i. Finally, the main takeaways from this are central DMFT equations, 2.28, 2.29, and 2.30. To make the calculations of solutions simpler, we reduce 2.28 and 2.29 to give

$$\langle \eta^a \eta^b \rangle_\eta = C^{ab} = \langle \phi(gh^a)\phi(gh^b) \rangle_\eta \tag{2.32}$$

where

$$h^a = h(t_a) = \int_{-\infty}^{t_a} dt_b \; e^{-(t_a - t_b)\eta(t_b)}. \tag{2.33}$$

Let us now define the relation between h^a and η^a as

$$\langle h_i^a h_i^b \rangle_\eta = \Delta^{ab}. \tag{2.34}$$

Then, from this and equation 2.32, we get the following relation between the field correlation Δ^{ab} and the activity correlation C^{ab}:

$$C^{ab} = \int \int \frac{d^2 h}{\sqrt{2\pi \det \Delta}} \exp\left[-\frac{1}{2} h^T \Delta^{-1} h \right] \phi(gh^a)\phi(gh^b) \tag{2.35}$$

where $h^T = (h^a, h^b)$. If we multiply equation 2.30 by itself and average over η, we obtain the relation:

$$(1 + \partial_a)(1 + \partial_b)\Delta^{ab} = C^{ab} \tag{2.36}$$

These two equations must be solved iteratively to obtain a self-consistent solution for C^{ab} and Δ^{ab}. Equation 2.35 expresses C^{ab} in terms of Δ^{ab}. This can be reduced to

$$\Delta - (\partial_\tau^2 \Delta) = C(\Delta; \Delta_0) \tag{2.37}$$

2.3 Solutions and Theoretical Predictions

Both the aforementioned mathematical formulations give us the same solutions for the system being in steady state. Let us therefore briefly go over both in a way that merges them.

The dynamical correlation functions exhibit time translation invariance, such that Δ^{ab} depends only on the time difference $\tau = t_a - t_b$.

Solving the DMFT equations is significantly aided by recognizing that for a fixed $\Delta_0 = \Delta(0)$, equation 2.37 can be thought of as describing the inertial dynamics of a particle moving under the influence of a potential $V(\Delta; \Delta_0)$, where V is as defined in 2.15, bringing us back to the expression 2.9. We can then obtain the conserved energies

$$E_c = \frac{1}{2}(\partial_\tau \Delta)^2 + V(\Delta; \Delta_0) \tag{2.38}$$

Since DMFT solutions must satisfy $\Delta_0 = \Delta(0)$ and $\frac{\partial \Delta}{\partial \tau}|_{\tau=0} = 0$, all solutions to equation 2.9 with energy $E_c = V(\Delta_0; \Delta_0)$ leading to bounded orbits are possible DMFT solutions of the form $\Delta = \Delta(\tau; \Delta_0)$. The qualitative behavior of the solutions can be inferred from the shape of the potential $V(\Delta, \Delta_0)$. The exact form of this potential, and hence the precise Δ dynamics it describes, depends on the specific choice of $\phi(x)$.

If $\partial^2 \Delta V(\Delta; \Delta 0)$ is positive at $\Delta = 0$, then the potential is a single well with a minimum at $\Delta = 0$. On the other hand, if $\partial^2 \Delta V(\Delta; \Delta 0)$ is negative at $\Delta = 0$, then the potential is a double well with two minima at nonzero values of Δ.

The two regimes - single-well and double-well potentials - are separated by the boundary where $E_c = 0$. At this boundary, $\Delta(\tau)$ decays monotonically to 0 as $\tau \to \infty$. When E_c reaches the minimum of

$$V(\Delta; \Delta_0),$$

the solution $\Delta(\tau)$ becomes time-independent. Above the curve $f(\Delta_0)$ in figure 2, there are no solutions with $\Delta_0 > 0$. Thus for $g < 1$, only the time-independent solution $\Delta = \Delta_0 = 0$ exists.
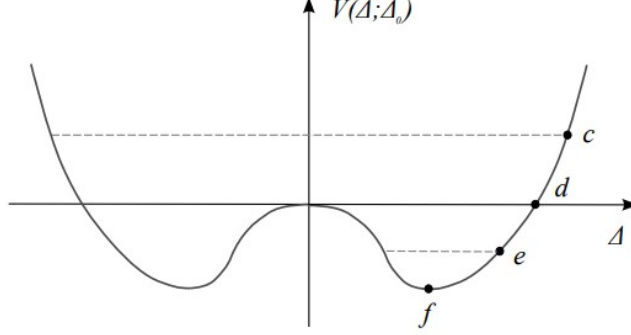

Figure 2: Double well potential $V(\Delta, \Delta_0)$.

Chaotic State

For $g > 1$, different scenarios appear. On the curve f, the energy E_Δ attains its minimum value and the solution is time-independent:

$$\Delta(\tau) = \Delta_0$$

On this curve, the network flows to a nonzero fix point characterized by a nontrivial distribution of h_i.

In the region below the curve f, E_Δ is larger than the minimum of $V(\Delta; \Delta_0)$ and $\Delta(\tau)$ becomes time-dependent. Here time-periodic solutions appear, either changing sign in one period below curve d or not between curves d and f. In either case, these solutions imply that the dynamical behavior of the network in the steady state is a limit cycle. On the curve d, corresponding to $E_\Delta = 0$ and separating the two types of periodic solutions, $\Delta(\tau)$ is not periodic and decays monotonically to 0 as $\tau \to \infty$. On this curve the dynamical behavior of the network is chaotic.

The existence of a bounded chaotic phase, in which the mean activity of the network remains finite and the trajectories of the local fields remain bounded, requires stability of the uniform mode. Unfortunately, a theoretical framework for analyzing stability in a time-dependent dynamical state is still lacking. However, in the linear case, simple arguments can be made for the existence of a chaotic solution [6]. Even though we lack a complete theory of stability for time-dependent dynamical states, the linearity of the model in this case allows us to argue that a bounded chaotic phase can exist. In the bounded chaotic phase:(i) the mean network activity remains finite and (ii) the local field trajectories remain bounded. This requires stability of the uniform mode, meaning small perturbations away from uniform activity do not diverge and amplify without bound.

While we lack a general theory of stability for time-dependent dynamical states, the linearity of the model in this case allows us to show that a bounded chaotic phase can exist, with stable, finite mean activity and bounded local field trajectories. Simple arguments based on the linear model point to the possibility of such a chaotic solution, even though we cannot perform a full stability analysis of the time-dependent state.

8

3 Simulation

We now try to simulate a large recurrent neural net and assess the effect of a small perturbation to the system as it proceeds into a chaotic state. Moreover, we will also compare the results with the state of the system at the beginning, $t = 0$.

3.1 Methodology

The steps taken to conduct the simulation are as follows:

1. Define the neural network model as in the paper: neurons i have activity h_i and are connected to others with weights J_{ij}.

2. Initialize the activities h_i and weights J_{ij} randomly, with J_{ij} drawn from a distribution that places the network near the chaotic transition point.

3. At each time step t, update the neuron activities:

$$h_i(t+1) = \tanh\left(\sum_j J_{ij} h_j(t)\right)$$

   This simulates network dynamics.

4. Run the simulation for many time steps until it reaches a steady state. At this point, the network will exhibit stable, non-chaotic activity.

5. At some time step t_0, apply a small perturbation to a subset of neurons: $h_i(t_0) \rightarrow h_i(t_0) + \epsilon$ for neurons in the perturbation set.

6. Continue running the simulation. Even though the initial perturbation ϵ is small, the network's activity will diverge over time from the unperturbed trajectory.

7. This demonstrates the sensitivity to initial conditions - a hallmark of chaos - that emerges near the transition point. The perturbation induces a long-lasting effect, causing the network activity to significantly diverge over time.

8. By varying J_{ij} to tune how close the network is to the transition point, the shift from stable to chaotic dynamics can be observed.

9. Key outputs would be: the network activity over time, comparison of perturbed and unperturbed trajectories, and calculation of the Lyapunov exponent to quantify chaos.

The Lyapunov exponent quantifies how fast small perturbations grow over time, indicating the presence of chaos. It is calculated as follows:

1. Perturb a subset of neurons by a small amount ϵ at some time step:

$$h_i(t_0) \rightarrow h_i(t_0) + \epsilon$$

2. Evolve the network dynamics from this perturbed state and from the original unperturbed state.

3. At each subsequent time step, calculate the distance d between the perturbed and unperturbed network states:

$$d = ||h_{perturbed} - h_{unperturbed}|| \tag{3.1}$$

4. Plot d as a function of time. For a chaotic system, d will increase exponentially: $d(t) \sim e^{\lambda t}$

The exponent λ in this exponential growth is the Lyapunov exponent. It quantifies the average exponential rate of divergence of nearby trajectories. A positive Lyapunov exponent indicates that small perturbations grow over time, rather than decay. This signifies sensitivity to initial conditions and chaos. A larger Lyapunov exponent corresponds to faster divergence of trajectories and more chaotic behavior.

So in this neural network model, by perturbing the system and measuring how fast the perturbation grows, we can calculate a Lyapunov exponent that indicates whether the system is exhibiting stable or chaotic dynamics. A positive exponent suggests chaos, while the magnitude indicates how chaotic the behavior is.

3.2   Results

After conducting the simulation as in [7], we obtain results that can be comparable to a network of $N \to \infty$ by having $N = 5000$ as the defined neural unit.

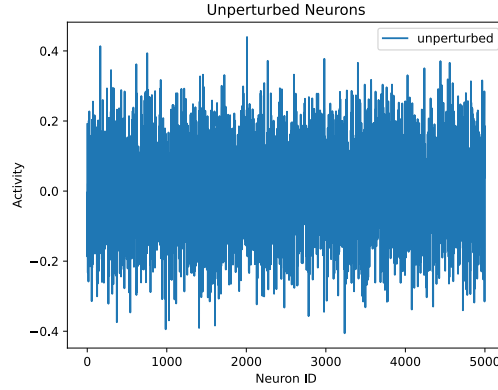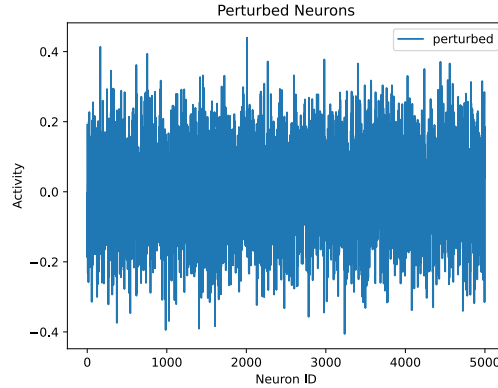**Figure 3:** Firing activity of unperturbed neurons, with Gaussian weights attached.

Figure 4: Firing activity of perturbed neurons, with Gaussian weights attached.

We add a small perturbation of $\epsilon = 0.1$ to the first few neurons and allow the system to go into chaos and then transition out of it. The firing activity of the perturbed and unperturbed neurons can be seen in figures 3 and 4. Not much can be inferred from these figures as they both look quite similar. However, let us now look at the distance d between the unperturbed and perturbed units in figure 5. Where the neurons are
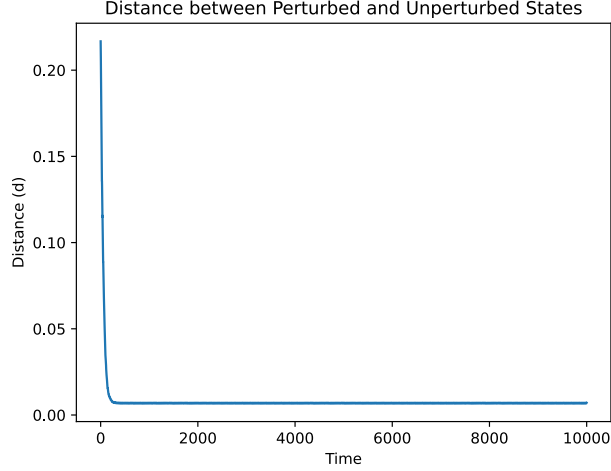
10

Figure 5: Distance d, calculated as in equation 3.1.

perturbed, we see the system having gone into chaos. Because a very small number of neurons have been perturbed, we see a steep change as the system transitions back into a stable state. When we calculate the Lyapunov exponent for this curve, we get

$$\text{Lyapunov exponent: } 0.0025843718747450106$$

This agrees with the predictions made, as it is a positive number and is small for our system, because of the very few number of neuronal units perturbed. As we can infer from the figure, when the system reaches a stable state again, the distance between perturbed and unperturbed neurons can be approximated to be 0.

4   Conclusion

In summary, the papers examine chaos in random neural networks theoretically, deriving analytical expressions for their dynamics and phase transition. The simulation method demonstrates the effect of perturbations close to the transition, revealing the underlying chaotic dynamics. It uses a range of analyses to detect and quantify chaos in the model.

References

[1] H. Sompolinsky, A. Crisanti, and H. J. Sommers, "Chaos in random neural networks," *Phys. Rev. Lett.*, vol. 61, pp. 259–262, Jul 1988. [Online]. Available: https://link.aps.org/doi/10.1103/PhysRevLett.61.259

[2] A. Crisanti and H. Sompolinsky, "Path integral approach to random neural networks," *Physical Review E*, vol. 98, no. 6, Dec 2018. [Online]. Available: https://doi.org/10.1103%2Fphysreve.98.062120

[3] G. Parisi, "Mean field theory of spin glasses: Statics and dynamics," Jun 2007. [Online]. Available: https://arxiv.org/abs/0706.0094

[4] T. Lancaster and S. Blundell, *Quantum Field Theory for the Gifted Amateur*. Oxford University Press, 2014.

[5] D. Cline, "9.2: Hamilton's principle of stationary action," *Physics LibreTexts*, Mar 2021. [Online]. Available: https://phys.libretexts.org/Bookshelves/Classical_Mechanics/ Variational_Principles_in_Classical_Mechanics_(Cline)/09%3A_Hamiltons_Action_Principle/9.02% 3A_Hamiltons_Principle_of_Stationary_Action

[6] J. Kadmon and H. Sompolinsky, "Transition to chaos in random neuronal networks," *Physical Review X*, vol. 5, no. 4, Nov 2015. [Online]. Available: https://doi.org/10.48550/arXiv.1508.06486

[7] [Online]. Available: https://github.com/hanis26/compneuro_proj_chaos